Ξ^0 and $\overline{\Xi}^0$ Polarization Measurements at 800 GeV/c.

E. Abouzaid[5], A. Alavi-Harati[13], T. Alexopoulos[13,†], M. Arenton[12], A.R. Barker[6,‡], L. Bellantoni[8], A. Bellavance[10], E. Blucher[5], G.J. Bock[8], S. Bright[5], E. Cheu[1], R. Coleman[8], M.D. Corcoran[10], B. Cox[12], A.R. Erwin[13], C.O. Escobar[4], R. Ford[8], A. Glazov[5], A. Golossanov[12], R.A. Gomes[4], P. Gouffon[11], K. Hanagaki[9], Y.B. Hsiung[8], H. Huang[6], D.A. Jensen[8], R. Kessler[5], K. Kotera[9], A. Ledovskoy[12], P.L. McBride[8], E. Monnier[5,*], K.S. Nelson[12], H. Nguyen[8], R. Niclasen[6], H. Ping[13], V. Prasad[5], X.R. Qi[8], E.J. Ramberg[8], R.E. Ray[8], M. Ronquest[12], T. Rooker[13], E. Santos[11], J. Shields[12], W. Slater[2], D.E. Smith[12], N. Solomey[5], E.C. Swallow[5,7], P.A. Toale[6], R. Tschirhart[8], C. Velissaris[13], Y.W. Wah[5], J. Wang[1], H.B. White[8], J. Whitmore[8], M. Wilking[6], B. Winstein[5], R. Winston[5], E.T. Worcester[5], M. Worcester[5], T. Yamanaka[9], E. D. Zimmerman[6], and R.F. Zukanovich[11]

(The KTeV Collaboration) **Physical Review Letters DRAFT V10.0**

[1] University of Arizona, Tucson, Arizona 85721
[2] University of California at Los Angeles, Los Angeles, California 90095
[3] University of California at San Diego, La Jolla, California 92093
[4] Universidade Estadual de Campinas, Campinas, Brazil 13083-970
[5] The Enrico Fermi Institute, The University of Chicago, Chicago, Illinois 60637
[6] University of Colorado, Boulder, Colorado 80309
[7] Elmhurst College, Elmhurst, Illinois 60126
[8] Fermi National Accelerator Laboratory, Batavia, Illinois 60510
[9] Osaka University, Toyonaka, Osaka 560 Japan
[10] Rice University, Houston, Texas 77005
[11] Universidade de São Paulo, São Paulo, Brazil 05315-970
[12] The Department of Physics and Institute of Nuclear and Particle Physics, University of Virginia, Charlottesville, Virginia 22901
[13] University of Wisconsin, Madison, Wisconsin 53706

The polarization of Ξ^0 and $\overline{\Xi}^0$ hyperons produced by 800 GeV/c protons on a BeO target at a fixed targeting angle of 4.8 mrad is measured by the KTeV experiment at Fermilab. Our result of 9.7% for Ξ^0 polarization shows no significant energy dependence when compared to a result obtained at 400 GeV/c production energy and at twice our targeting angle. The polarization of the $\overline{\Xi}^0$ is measured for the first time and found to be consistent with zero. We also examine the dependence of polarization on production p_t.

PACS numbers: 13.30.Ce, 14.20.Jn

(May 30, 2006)

I. INTRODUCTION

Although there is an abundance of data on the subject of hyperon polarization in hadroproduction, there is still no theory that can correctly explain these data. The discovery of hyperon polarization at Fermilab was unexpected [1]. The simplest application of perturbative Quantum Chromodynamics (pQCD) assuming massless quarks predicts no polarization effects. If one considers a theory where both proton valence and sea quarks can be polarized in the collision, then some correlation between SU(6) wavefunctions and the measured sign and magnitude of polarization is possible [2]. But the pattern of polarization for the various hyperons is far more complex than this theory can handle. More significantly, no theory can explain the observation of anti-hyperon polarization in high energy collisions. Considering the latter point, it is important to measure the polarization for all the anti-hyperons. This letter reports on measurements of the energy dependence in Ξ^0 polarization and the first measurement of polarization in $\overline{\Xi}^0$ production by the KTeV experiment at Fermilab, using the decay $\Xi^0 \to \Lambda\pi^0$.

The production and polarization of hyperons and anti-hyperons have historically been measured as a function of hyperon momentum (p), production angle (θ), beam energy (p_{beam}) and target material [3,4]. Results are typically reported as a function of the combined variables of transverse momentum, $p_t = p\ sin\theta$, and longitudinal momentum fraction, also called Feynman x, $x_F = p/p_{beam}$. For a fixed angle of hyperon production, as in the data reported here, the two variables are proportional to each other. We report our polarization results as a function of p_t.

Experiments have shown a wide variety of polarization behavior with respect to p_t and x_F[2,4-8]. Reference [8] reported an equal polarization between Λ at 800 GeV/c with 4.8 mrad targeting and at 400 GeV/c with 9.6 mrad targeting. In contrast, measurements of the Σ^+ and $\overline{\Sigma}^-$ polarization [6] have shown a decrease of polarization for 800 GeV/c production when compared to 400 GeV/c prodcution. And finally, an increase in polarization of the Ξ^- as a function of the beam energy, from 400 GeV/c to 800 GeV/c, has been measured [7].

There is not as much polarization data for anti-

hyperons. Most are produced with no polarization. Exceptions are 800 GeV/c production of $\overline{\Xi}^+$ in E756 [9] and $\overline{\Sigma}^-$ in E761 [6]. In these experiments, the anti-hyperons were produced with the same magnitude and sign of polarization as their hyperon counterparts.

II. BEAM

The data discussed in this letter were obtained by the KTeV experiment at Fermilab. It used an 800 GeV/c proton beam with a 19 second spill of $\sim 5 \times 10^{12}$ protons once per minute. The 1.1 interaction length (30 cm) BeO target was targeted at a mean downward angle of 4.80 ± 0.15 mrad with a rms spread of $\pm$ 0.24 mrad. Downstream of this target was a set of sweeping magnets used to remove charged particles. At this targeting angle and beam energy, then $x_F = 0.26 p_t (GeV/c)$

A right handed KTeV coordinate system was defined with the z-axis along the hyperon beam momentum ($\mathbf{p}_\Xi$) and the y-axis along the vertical direction. For strong production processes polarization should be normal to production plane. Polarization is defined as positive when it is along the normal unit vector $\hat{n} = \hat{p}_p \times \hat{p}_\Xi$, where $\hat{p}_p$ and $\hat{p}_\Xi$ are unit vectors along the incident proton beam momentum and along the produced Ξ momentum respectively. The $\hat{n}$ vector is along the negative $\hat{x}$ direction of the KTeV coordinate system.

Located in the target area, the neutral beam sweeping magnets had their magnetic fields oriented in the vertical ($\hat{y}$) direction. Their combined field value was set such that the Ξ^0 spin was precessed into the $\hat{z}$-direction. By switching the polarity of a final rotational magnet (RoM), whose field was parallel to the $\hat{x}$-direction, the Ξ^0 spin was finally precessed alternately into the positive and then negative $\hat{y}$-axis approximately once a day. We used the known value of the Ξ^0 magnetic moment [10] to set the magnet field values.

A series of collimators defined two nearly parallel neutral beams that entered the KTeV apparatus 94 m downstream from the target. The composition of the beams was mainly neutrons and K_L's, with a small admixture of Λ's and Ξ's.

III. DETECTOR

The KTeV apparatus consisted of a 65 m vacuum ($\sim 10^{-6}$ Torr) decay region followed by a charged particle spectrometer. This spectrometer consisted of a dipole analysis magnet (AnM) with two drift chambers on either side of it. To reduce multiple scattering, helium-filled bags occupied the spaces between the drift chambers. For the data discussed here, the magnetic field imparted a 205 MeV/c horizontal momentum component to charged particles. The AnM field direction was reversed approximately once a day. The momentum resolution of the spectrometer was $\sigma(p)/p = 0.38\% \oplus 0.016\% \, p(\mathrm{GeV/c})$, where the sum is in quadrature.

The charged particle spectrometer was followed by a ($1.9 \times 1.9\,\mathrm{m}^2$) electromagnetic calorimeter (ECAL), which consisted of 3100 pure CsI crystals. After calibration, the ECAL energy resolution was better than 1% for an electron momentum between 2 and 60 GeV/c. The position resolution was 1 mm.

Nine photon veto assemblies detected particles leaving the fiducial volume. Two scintillator hodoscopes in front of the ECAL were used to trigger on charged particles. Another scintillator plane (hadron-anti), located behind both the ECAL and a 10 cm lead wall, acted as a hadron shower veto. The hodoscopes and the ECAL detectors had two holes and the hadron-anti had a single hole to let the neutral beams pass through without interaction. Charged particles passing through these holes were detected by 16×16 cm^2 scintillators (hole counters) located along each beam line in the hole region just downstream of the hadron-anti. Two steel walls, with two sets of hodoscopes, acted as a muon identifier.

Decays of the type $\Xi^0 \to \Lambda\pi^0 (\overline{\Xi}^0 \to \overline{\Lambda}\pi^0)$ produce a high momentum (>100 GeV/c) positive(negative) track proton(antiproton) which remains in or near the neutral beam region. In addition there is a second lower momentum $\pi^-(\pi^+)$ track, and two ECAL energy clusters not associated with tracks that correspond to the two photons from the π^0 decay. Our trigger was based on these signatures.

IV. DATA ANALYSIS

We reconstruct $\Xi^\circ \to \Lambda\pi^\circ$ decays and the antihyperon counterpart from both charged track and ECAL cluster quantities. From the energy and position of the photons entering the calorimeter, the position of the Ξ^0 vertex along the beam is calculated as $(\Delta z) = (\delta/m_{\pi^\circ})\sqrt{E_1 E_2}$, where Δz is the distance of the vertex from the ECAL position, E_1 and E_2 are the energies of the photons, δ is the distance between the photons at the calorimeter and m_π^0 is the known [10] π^0 mass. The reconstructed proton and π^- momentum vectors, in the Ξ^0 case, are combined to form the Λ momentum vector, which defines its flight path. The Λ flight path is extrapolated backwards to the point where it intersects the z-plane of the Ξ^0 decay. This intersection yields the x and y coordinates of the Ξ^0 decay vertex. Further details of the KTeV hyperon trigger and analysis cuts used to reduce background can be found in a previous paper [11,12]

For the selected data, Fig. 1 shows the effect on the reconstructed Ξ^0 mass after all cuts for various combinations of analysis magnet and spin rotational magnet

settings. The remaining background levels for the $\Lambda\pi^0$ mass peaks are less than 0.5%.

The Ξ^0 or $\bar{\Xi}^0$ polarization was determined by first splitting our data into two oppositely polarized samples (RoM> 0, RoM< 0) and then calculating the direction cosines $(\cos\theta_x, \cos\theta_y, \cos\theta_z)$ of the Λ momentum vector in the Ξ^0 rest frame. For a sample of decays where the Ξ^0 has an average polarization P, the normalized direction cosine distribution $(f_\pm)$ is

$$f_\pm(\cos\theta_k) = \frac{dN}{d\cos\theta_k} = A(\cos\theta_k)(1 \pm \alpha_{\Xi^0} P_k cos\theta_k) \quad (1)$$

where $k = x, y, z$ and P_k is the k-component of polarization P along the $\hat{k}$-axis. $A(\cos\theta_k)$ is a function that describes the experimental acceptance for Ξ^0 decays as a function of the Λ direction cosine and is a strong function of the analysis magnet (AnM) setting for the $cos\theta_x$ distribution. α_{Ξ^0} is the known Ξ^0 decay asymmetry parameter [10]. The quantity f_+ (f_-) is the fraction of the up (down) precession sample for a given value of $\cos\theta_k$.

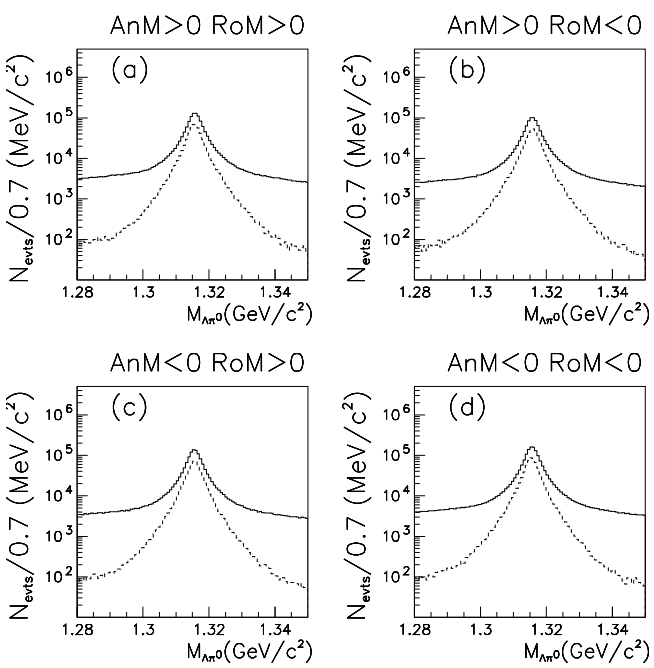

FIG. 1. Reconstructed cascade mass from data for various Analysis (AnM) and Rotational Magnet (RoM) conditions, before (solid line) and after (dash line) the application of the analysis cuts.

The anti-symmetric ratio:

$$R(\cos\theta_k) = \frac{(f_+ - f_-)}{(f_+ + f_-)} = \alpha_{\Xi^0} P_k \cos\theta_k \quad (2)$$

has a slope with respect to $\cos\theta_k$ which gives the asymmetry $\alpha_{\Xi^0} P_k$, from which the polarization component P_k is obtained. As long as the acceptance of the detector is factorable and does not vary rapidly with time, it cancels out in the ratio. Figure 2 shows a comparison between the Λ direction cosine distributions for the two RoM rotational magnet settings. We have combined the data from the two AnM settings for each RoM setting in this figure. As can be seen, the pairs of distributions are essentially identical in the $\hat{x}$ and $\hat{z}$ directions. In the $\hat{y}$ direction, however, the two distributions are clearly different, showing the effect of the Ξ^0 polarization on the Λ decay distribution.

These effects are even more visible in the plots of the ratio defined in Eq. (2) and are shown in Fig. 2. Linear fits to these graphs extract the polarization components P_x, P_y, P_z. The extracted fitted slopes for the $\hat{x}$ and $\hat{z}$ directions are consistent with zero ($P_x = P_z = -0.001 \pm 0.003_{stat}$), while the $\hat{y}$ slope shows a clear indication of the polarization effect. After taking into account acceptance differences of the order of 10%, using Monte Carlo generated events [11,12], the extracted polarization in the $\hat{y}$-direction is $P_y = -0.097 \pm 0.007_{stat} \pm 0.013_{sys}$. The systematic error is based on the largest value for polarization seen in the $\hat{x}$ and $\hat{z}$ directions. We also checked that varying analysis cuts by 10% of their nominal values had no significant effect on polarization values. Monte Carlo reconstructed values for polarization track linearly with input polarization, at a level much better than the stated systematic error. The error on α_{Ξ^0} is included in the P_y result.

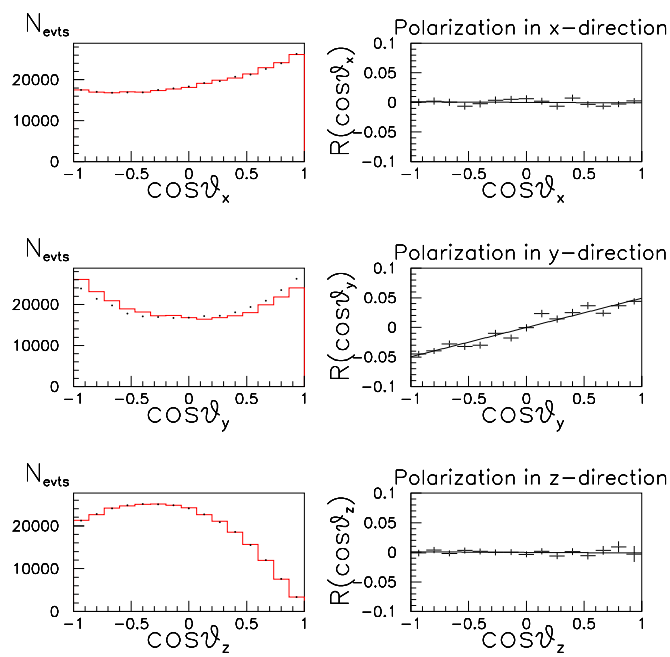

FIG. 2. Normalized direction cosine distributions $f_\pm$ (RoM> 0/RoM< 0) in $\hat{x}, \hat{y}, \hat{z}$ direction for $\Xi^0 \to \Lambda\pi^0$ decays, on the left. Histogram and dots represent the f_+ and f_- distributions respectively. Graphs on the right, show the ratio $R(\cos\theta_k)$. Error bars are statistical only.

We carried out a polarization analysis for the $\overline{\Xi}^0$ decay mode as well. Fig. 3 shows a comparison between the $\overline{\Lambda}$ direction cosine distributions for the two RoM rotational magnet settings. As can be seen, the pairs of distributions are essentially identical in all directions, indicating no statistically significant polarization effect for the $\overline{\Xi}^0$. Taking into account the small acceptance effect, the extracted y-component polarization is $P_y = 0.000 \pm 0.013_{stat} \pm 0.013_{sys}$. The P_x and P_z results remain consistent with zero.

To study the detailed momentum dependence of polarization in Ξ^0 and $\overline{\Xi}^0$ production we divided the data into transverse momentum bins. For each bin, the corresponding polarization was calculated. Results are shown in Fig. 4 as a function of the transverse momentum for Ξ^0 and $\overline{\Xi}^0$. Errors shown are statistical only.

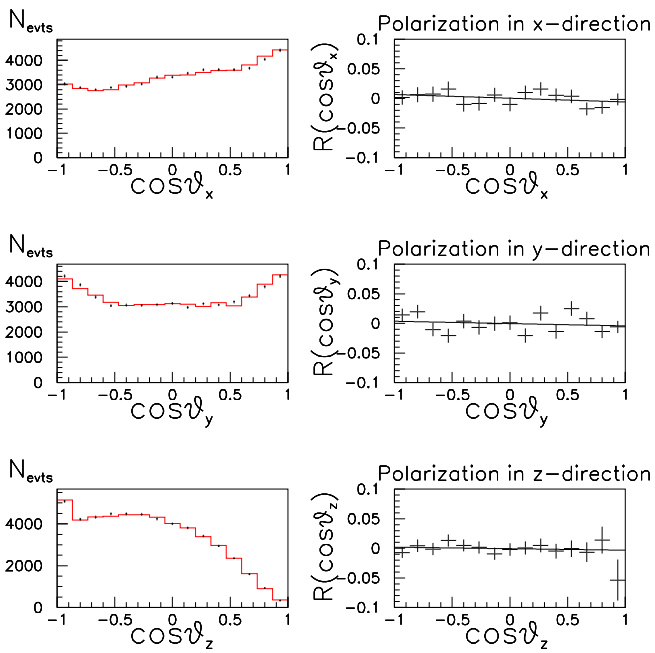

FIG. 3. Normalized direction cosine distributions $f_\pm$ in $\hat{x}, \hat{y}, \hat{z}$ for $\overline{\Xi}^0 \to \overline{\Lambda}\pi^0$ decays, on the left. Histogram is the f_+ and dots represent the f_- distribution. Graphs on the right, show the ratio $R(\cos\theta_k)$. Error bars are statistical only.

Comparable data from a past Fermilab experiment [4] have been superimposed on this plot. Those Ξ^0 data had a targeting angle of 9.8 mrad, approximately twice our targeting angle, a proton beam energy of 400 GeV, half of our KTeV energy, and a similar target material (Be). For a given value of p_t, these data samples have the same x_F value as the data presented here, and are therefore directly comparable. No significant change in Ξ^0 polarization is seen between the two production energies of 400 and 800 GeV. Also, the Λ polarization from the Fermilab experiment E799I [8] is shown, produced with the same targeting angle of 4.8 mrad and proton beam energy of 800 GeV. There is a striking similarity between Λ and Ξ^0 polarization.

V. CONCLUSION

In conclusion, we have measured the polarization of the Ξ^0 and $\overline{\Xi}^0$ hyperons produced by 800 GeV/c protons at a fixed targeting angle of 4.8 mrad for the first time. Comparing the measured polarization values for the Ξ^0 decay mode with those determined previously for production at 400 GeV/c and a targeting angle of 9.8 mrad, we find there is no energy dependence in Ξ^0 production. We also find no statistically significant polarization for the $\overline{\Xi}^0$ at 800 GeV/c. This is in contrast to two previous reports for other anti-hyperon polarizations [6,9].

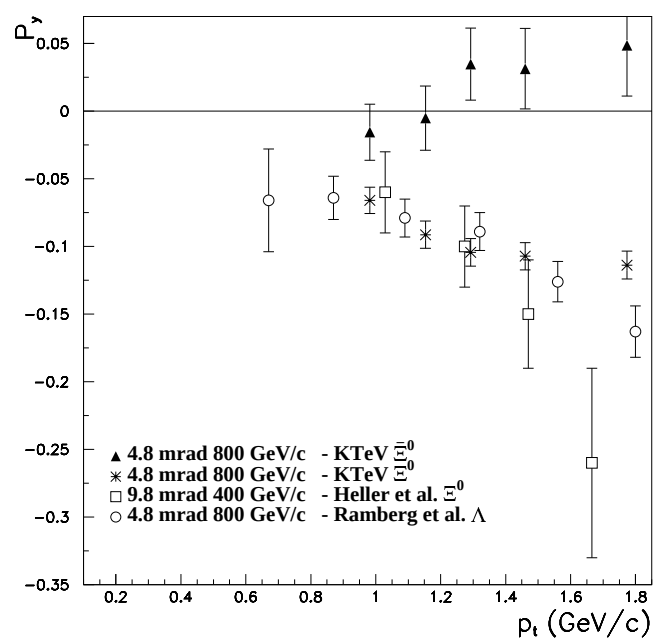

FIG. 4. Ξ^0 and $\overline{\Xi}^0$ polarization versus production transverse momentum p_t. For comparison, Ξ^0 data [4] from 400 GeV/c and Λ data [8] from 800 GeV/c are also shown.

VI. ACKNOWLEDGMENTS

We would like to thank L. Pondrom for helpful discussions. We gratefully acknowledge the support of the technical staffs of all participating institutions. This work was supported in part by the US Department of Energy, The National Science Foundation, The Ministry of Education and Science of Japan, Fundação de Amparo a Pesquisa do Estado de São Paulo-FAPESP, Conselho

Nacional de Desenvolvimento Cientifico e Tecnologico-CNPq and CAPES-Ministerio da Educação.

* On leave from C.P.P. Marseille/C.N.R.S., France.
† Electronic address: talexopo@cern.ch
‡ deceased

[1] G. Bunce *et al.*, Phys. Rev. Lett. 36, 1133 (1976).
[2] L. Pondrom, Phys. Rep. **122**, 57 (1985).
[3] K. Heller, in *Spin and Polarization Dynamics in Nuclear and Particle Physics*, edited by A. Barut, Y Onel and A. Penzo (World Scientific, New Jersey, 1990), 36.
[4] K. Heller *et al.*, Phys. Rev. Lett. **51**, 2025 (1983).
[5] Peter S. Cooper, "Hyperon Beam Physics", Fermilab-Conf-96/063, Fermi National Laboratory, March 1996 (unpublished).
[6] A. Morelos *et al.*, Phys. Rev. Lett. **71**, 2172 (1993).
[7] J. Duryea *et al.*, Phy. Rev. Lett. **67**, 1193 (1991).
[8] E.J. Ramberg *et al.*, Phys. Lett. B **338**, 403 (1994).
[9] P. M. Ho *et al.*, Phys. Rev. D **44**, 3402 (1991).
[10] S. Eidelman *et al.* (Particle Data Group), Phys. Lett B **592**, 1 (2004).
[11] A. Alavi-Harati *et al.*, Phy. Rev. Lett. **87**, 132001 (2001).
[12] A. Alavi-Harati *et al.*, Phy. Rev. Lett. **82**, 3751 (1999).